

This is a copy of the published version, or version of record, available on the publisher's website. This version does not track changes, errata, or withdrawals on the publisher's site.

Modeling dark- and light-induced crystal structures and single-crystal optical absorption spectra of ruthenium-based complexes that undergo SO₂-linkage photoisomerization

Apoorv Jain, Jacqueline M. Cole, Álvaro Vázquez-Mayagoitia, and Michael G. Sternberg

Published version information

Citation: A Jain et al. Modeling dark- and light-induced crystal structures and single-crystal optical absorption spectra of ruthenium-based complexes that undergo SO₂-linkage photoisomerization. *J Chem Phys* 155 (2021): 234111

DOI: [10.1063/5.0077415](https://doi.org/10.1063/5.0077415)

This article may be downloaded for personal use only. Any other use requires prior permission of the author and AIP Publishing.

This version is made available in accordance with publisher policies. Please cite only the published version using the reference above. This is the citation assigned by the publisher at the time of issuing the APV. Please check the publisher's website for any updates.

This item was retrieved from **ePubs**, the Open Access archive of the Science and Technology Facilities Council, UK. Please contact epublications@stfc.ac.uk or go to <http://epubs.stfc.ac.uk/> for further information and policies.

Modeling dark- and light-induced crystal structures and single-crystal optical absorption spectra of ruthenium-based complexes that undergo SO₂-linkage photoisomerization

Cite as: J. Chem. Phys. **155**, 234111 (2021); <https://doi.org/10.1063/5.0077415>

Submitted: 02 November 2021 • Accepted: 10 November 2021 • Accepted Manuscript Online: 15 November 2021 • Published Online: 20 December 2021

Apoorv Jain,  Jacqueline M. Cole, Álvaro Vázquez-Mayagoitia, et al.



View Online



Export Citation



CrossMark

ARTICLES YOU MAY BE INTERESTED IN

[Ultrafast sorting: Excimeric \$\pi\$ - \$\pi\$ stacking distinguishes pyrene-N-methylacetamide isomers on the ultrafast time scale](#)

The Journal of Chemical Physics **155**, 234304 (2021); <https://doi.org/10.1063/5.0072785>

[On-the-fly adiabatically switched semiclassical initial value representation molecular dynamics for vibrational spectroscopy of biomolecules](#)

The Journal of Chemical Physics **155**, 234102 (2021); <https://doi.org/10.1063/5.0075220>

[High-Q plasmonic nanowire-on-mirror resonators by atomically smooth single-crystalline silver flakes](#)

The Journal of Chemical Physics **155**, 234202 (2021); <https://doi.org/10.1063/5.0074387>



Chemical Physics Reviews

First Articles Now Online!

READ NOW >>>



Modeling dark- and light-induced crystal structures and single-crystal optical absorption spectra of ruthenium-based complexes that undergo SO₂-linkage photoisomerization

Cite as: J. Chem. Phys. 155, 234111 (2021); doi: 10.1063/5.0077415

Submitted: 2 November 2021 • Accepted: 10 November 2021 •

Published Online: 20 December 2021



View Online



Export Citation



CrossMark

Apoorv Jain,^{1,2} Jacqueline M. Cole,^{1,2,3,4,a)}  Álvaro Vázquez-Mayagoitia,⁴ and Michael G. Sternberg⁴

AFFILIATIONS

¹Cavendish Laboratory, Department of Physics, University of Cambridge, J. J. Thomson Avenue, Cambridge CB3 0HE, United Kingdom

²Department of Chemical Engineering and Biotechnology, University of Cambridge, West Cambridge Site, Philippa Fawcett Drive, Cambridge CB3 0AS, United Kingdom

³ISIS Neutron and Muon Source, STFC Rutherford Appleton Laboratory, Harwell Science and Innovation Campus, Didcot OX11 0QX, United Kingdom

⁴Argonne National Laboratory, 9700 S Cass Avenue, Lemont, Illinois 60439, USA

^{a)}Author to whom correspondence should be addressed: jmc61@cam.ac.uk

ABSTRACT

A family of coordination complexes of the type $[\text{Ru}(\text{SO}_2)(\text{NH}_3)_4\text{X}]^{m+}\text{Y}_n^-$ ($m, n = 1$ or 2) exhibit optical switching capabilities in their single-crystal states. This striking effect is caused by the light-induced formation of SO₂-linkage photoisomers, which are metastable if kept at suitably cool temperatures. We modeled the dark- and light-induced states of these large crystalline complexes via plane-wave (PW)- and molecular-orbital (MO)-based density functional theory (DFT) and time-dependent DFT in order to calculate their structural and optical properties; the calculated results are compared with experimental data. We show that the PW-DFT-based periodic models replicate the structural properties of these complexes more effectively than the MO-DFT-based molecular-fragment models, observing only small deviations in key bond lengths relative to the experimentally derived crystal structures. The periodic models were also found to more effectively simulate trends seen in experimental optical absorption spectra, with optical absorbance and coverage of the visible region increasing with the formation of the photoinduced geometries. The contribution of the metastable photoisomeric species more heavily focuses on the lower-energy end of the spectra. Spectra generated from the molecular-fragment models are limited by the geometry of the fragment used and the number of excited-state roots considered in those calculations. In general, periodic models outperform the molecular-fragment models owing to their ability to better appreciate the periodic phenomena that are present in these crystalline materials as opposed to MO approaches, which are finite methods. We thus demonstrate that PW-DFT-based periodic models should be considered as a more than viable method for simulating the optical and electronic properties of these single-crystal optical switches.

Published under an exclusive license by AIP Publishing. <https://doi.org/10.1063/5.0077415>

I. INTRODUCTION

Crystalline systems that display solid-state linkage photoisomerization stand to yield new applications in nanophotonics¹ and quantum technology.² Materials that produce molecular crosstalk are of particular interest as they hold potential for optical actuation,³ optical signal processing, and optomechanical functions.^{4–7}

One such family of materials is a set of ruthenium-sulfur dioxide coordination complexes that exhibit a rare case of controllable and reversible nano-optical switching in the crystalline state, thus behaving as single-crystal optical actuators.^{8–20} Their behavior showcases the possibility for single crystals to operate as nanotechnological devices themselves, potentially overcoming complications that are common in device processing.

Their functional origins stem from optically accessible energy levels of SO₂-linkage photoisomers that can be realized within a crystal lattice and maintained in a long-lasting metastable state once photoinduced. The photoisomers represent a solid-state binary switch, whereby the photoinduced metastable “light state” signifies a 1 and the original “dark state” signifies a 0. The general formula for this series of complexes is [Ru(SO₂)(NH₃)₄X]Y (hereafter referred to as [RuSO₂] complexes), where X is the ligand in the *trans* position with respect to the photoisomerizable SO₂ ligand and Y is the counterion. Photocrystallographic studies^{21–25} have shown that upon photoisomerization, which is primarily induced by the absorption of visible light, the SO₂ ligand can occupy one of two metastable photoinduced coordination modes: the O-bound (η^1 -OSO) state and the thermally more stable side-on η^2 -(OS)O state (Fig. 1). These two photoisomeric configurations may coexist in the light-induced crystal structure in different fractions along with the S-bound dark state (η^1 -SO₂).

This family of complexes has largely been studied experimentally, with new complexes having been discovered and characterized mainly via photocrystallography^{21–25} and single-crystal optical absorption spectroscopy.²⁶ This has resulted in highly accurate structural data and optical absorption spectra for both the dark and light states of these complexes. However, a purely experiment-based materials-discovery pathway is not viable for an extensive large-scale study of the various properties and structural intricacies of these complexes. It is thus desirable to add a computational element to this materials-discovery pathway by conducting electronic-structure calculations. However, the simulation of such crystalline materials is quite challenging, as they are large (>100 atoms per unit cell), solid, extended, photosensitive crystalline materials with heavy elements, long-range electrostatic (LRES) forces, and metal-based charge-transfer properties. They also exhibit a rare ability to form coexisting long-lasting metastable states upon photoactivation, which are ground states rather than excited states. The “dark” and “light” states of these complexes are distinct ground states that differ in geometry and coordination and must be modeled independently. Both dark- and light-state phenomena are present within a crystal lattice, and so this is inherently

a crystalline problem. Any effective computational approach will require an appreciation of the periodic nature of these systems and their properties. The success of the models, created by electronic-structure calculations, can be gauged by their ability to accommodate these complications and effectively simulate empirically calculated geometric and optical properties that match experimental results.

The most effective method of obtaining the optical response of bulk solids involves solving the Bethe–Salpeter equation (BSE),^{27–30} which accounts for the electron–hole interaction, on top of the many-body GW method.^{31,32} However, GW-BSE is computationally very intensive, and it does not scale well for large periodic systems. A computationally more feasible method is the quantum mechanics/molecular mechanics (QM/MM) approach.³³ Here, the electronic structure is partitioned into two sections: the QM part, which utilizes *ab initio* calculations, and the MM part, which models any long-range forces and the like via a force-field. One such study on this family of [RuSO₂] complexes was conducted by Aono and Sakaki,³⁴ who surveyed the thermal isomerization potential energy surface (PES) and studied the effects of short- and long-range forces on the SO₂ ligand. This study highlights the importance and difficulties associated with accurately defining the two regions. Various approximations have to be made when constructing the QM region, making it difficult to accurately model the LRES forces. Describing the MM region is also not trivial since it requires certain estimations of where and how these forces localize, which may not always be well understood. The details required in QM/MM make conducting optical calculations complicated and often computationally arduous.

Higher-order techniques, such as QM/MM and GW/BSE, also tend to require significant user input and lend themselves to potential bias being introduced by a personal understanding of the system at hand. “Black-box” techniques are thus preferred, particularly for large complex systems. Thereby, time-dependent density functional theory (TDDFT) is the “go-to” technique for calculating the optical properties of large complex periodic systems since it is able to provide a more sustainable trade-off between accuracy, simplicity, and computational load.^{27,28} This is despite the

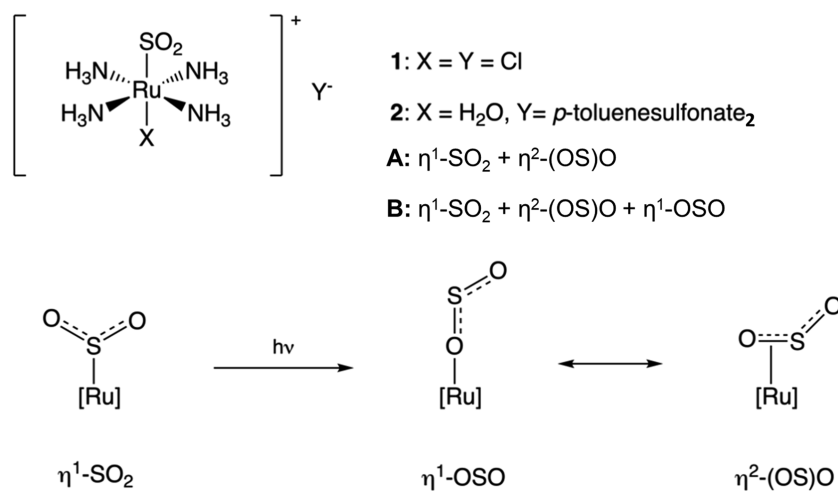


FIG. 1. Chemical structures of complexes 1 and 2 (top) together with the dark state (η^1 -SO₂) and photoinduced [η^1 -OSO and η^2 -(OS)O] configurations (bottom). Complexes of set A only form the η^2 -(OS)O state, whereas complexes of set B form both η^2 -(OS)O and η^1 -OSO.

well-established shortcomings of DFT when dealing with such systems.^{27,28}

Within the scope of TDDFT calculations, molecular-orbital molecular-fragment TDDFT^{35–37} “molecular-fragment” models are the typically preferred DFT-based methodology for calculating the optical properties of large extended systems owing to the large variety of Gaussian basis sets that are available. A MO-based molecular-fragment study by Kovalevsky *et al.*¹⁵ has been conducted on this family of [Ru–SO₂] complexes. However, it did not focus on the optical properties of these crystalline systems; rather, it focused on the evaluation of the various SO₂ ligand configurations by studying the surrounding PES.¹⁵ Significantly, these calculations were conducted only on the cations of these [RuSO₂] complexes, where **X** = Cl and H₂O.¹⁵ This study was thus not able to examine these complexes holistically because MO-based approaches are designed to treat finite molecules and, therefore, struggle to simulate periodic phenomena. Extended systems have to be modeled via a “molecular fragment” to mimic periodicity and to somewhat consider the effects of periodic phenomena, such as LRES forces. The size of the molecular fragment then becomes a decisive factor in the quality and complexity of these models. When heavy atoms are present, where polarization and diffuse effects are particularly important, extremely detailed basis sets are also required in order to achieve reasonable levels of accuracy, hence further increasing computational load (especially memory requirements). Although MO-based approaches do allow for the targeted analysis of certain regions of interest, they are unable to effectively appreciate the periodic character of extended systems due to their finite nature.

In contrast, plane-wave (PW) DFT is a periodic approach that is inherently constructed to treat systems with periodicity, and is the designated DFT-based methodology when dealing with extended materials.^{38,39} It is a viable alternative to molecular-fragment models since it is better equipped to handle periodic phenomena while offering the same computational savings. Interestingly, periodic approaches are often overlooked when the prediction of optical properties is required even though they have widespread use when calculating ground-state properties of large extended systems. Phillips *et al.*¹⁸ have conducted a PW-DFT based periodic study on this family of [RuSO₂] complexes, whereby they evaluated the PES of the SO₂ ligand and investigated the influence of the crystalline environment effects on its various configurations. However, this study could not comprehensively examine these [RuSO₂] complexes since periodic calculations were conducted with constrained geometries and lacked an evaluation of the optical response of these systems. There is thus a need to holistically model these [RuSO₂] complexes and their electronic, structural, and optical properties.

To that end, this study evaluates the ability of PW-DFT based periodic models to effectively simulate the experimentally determined single-crystal diffraction and optical absorption spectra of these crystalline [RuSO₂] complexes. Calculations were conducted on four periodic crystal structures of two complexes: (i) two variants of the simplest complex in this series where **X** = **Y** = Cl; **1A** only forms the η^2 -(OS)O photoisomer, whereas **1B** forms both η^1 -OSO and η^2 -(OS)O photoisomers; and (ii) two variants of the thermally most stable complex in this [RuSO₂] series, where **X** = H₂O and **Y** = *p*-tosylate; **2A** only forms the η^2 -(OS)O photoisomer, whereas **2B**

forms both η^1 -OSO and η^2 -(OS)O photoisomers. All four structures behave as photoswitches. Initially, structural relaxation calculations for all dark and light states were conducted in order to reproduce the experimentally determined crystal-structure geometries. These optimized structures were then used to simulate optical absorption spectra via linear-response TDDFT to replicate features seen in their experimentally determined single-crystal absorption spectra. The same series of calculations was also conducted via molecular-fragment models that comprise the four structures of the same two complexes to provide a comparison between periodic and MO-based approaches. An MO-based analysis of the optical results was also undertaken in order to study the orbitals that are involved in the various metal-based charge-transfer transitions. This study thereby showcases the strength of the periodic approach in modeling these extremely complex systems and why periodic models should be considered as a viable alternative to molecular-fragment models for studying the structural and optical properties of these large periodic materials that exhibit single-crystal optical actuation via linkage photoisomerism.

II. DFT MODELS AND COMPUTATIONAL METHODOLOGY

A. Optimized DFT models and reproduction of experimental structures

1. Periodic models

All periodic calculations were conducted using 6.4 version of the *Quantum Espresso*^{40,41} (QE) suite of codes, as available on the Theta machine at the Argonne Leadership Computing Facility (ALCF), IL, USA. The unit cells of the experimentally determined crystal structures^{15,16,26} were used as the starting geometries for all four structures of these complexes (with 88 atoms in the unit cells for **1A** and **1B** and 118 atoms for **2A** and **2B**). The ideal functional and pseudopotential pairing was determined in an iterative manner. A series of generalized gradient approximation (GGA) functionals were trialed along with two Perdew–Burke–Ernzerhof (PBE)-based hybrid functionals, PBE0⁴² and HSE.⁴³ For the hybrid functionals, PBE0 and HSE, several different exact-exchange fractions and screening parameters were explored. However, PBEsol⁴⁴ emerged as the ideal candidate, given that the spectra generated via GGA functionals⁴⁵ were much more similar to experimentally derived reference spectra, compared to those produced via their hybrid counterparts [see the [supplementary material](#) (Fig. S1.3) for further details]. Owing to the success of PBEsol as a functional for our benchmarking calculations, PBEsol-based scalar relativistic Optimized Norm-Conserving Vanderbilt Pseudopotentials (ONCVP-SPs)⁴⁵ were employed for our lead calculations. This pairing of functionals and potentials yielded improved spectral shape, removing unwanted features. For a detailed description of the pseudopotential choice, the reader is referred to the [supplementary material](#). This setup was used for all four crystal structures of the two complexes along with the Grimme DFT-D2 method,⁴⁶ which was used to account for van der Waals interactions, which are crucially important in these materials.

Having settled on the modeling parameters that are common to all ten photoisomeric structures of these two complexes, the PW energy cutoffs were determined, and Brillouin zone sampling was

undertaken. Each system required its own corresponding PW energy cutoff value. In all cases, the charge-density cutoff was four times larger than the energy cutoff. The required level of Brillouin zone sampling was determined using the Monkhorst–Pack scheme.⁴⁷ The energy cutoff values and Brillouin zone sampling used for calculations on each crystal structure of the two complexes, along with convergence details, can be found in the [supplementary material](#) (Table S2). As expected, these large systems require few k-points to be adequately described, which shows that they are not very k-point sensitive.

With the simulation parameters set, geometry optimizations were conducted on all dark and light states of all four structures of the two complexes. The experimentally determined crystal structures of the dark- and light-induced states were used as the starting geometries. No constraints were placed on any atoms, except for the η^2 -(OS)O isomer of **1B** where the SO₂–Ru–Cl axis had to be fixed to ensure that the geometry remained in the η^2 -(OS)O configuration (for details, see Sec. III A). The geometry of each structure was considered to have converged when the energy between successive optimization steps was within 10^{−4} Ry and the forces were within 10^{−3} Ry/bohr. The unit-cell parameters were fixed to experimental values throughout the simulation. The optimized geometries can be found in the [supplementary material](#).

2. Molecular-fragment models

All calculations were conducted using the NWChem software⁴⁸ on the carbon cluster, the high-performance computing facility at the Center for Nanoscale Materials at Argonne National Laboratory, IL, USA. The starting geometries used were based on the experimentally determined dark- and light-induced crystal structures for both types of complexes. The experimentally determined unit cell parameters and geometries were expanded to recreate complete molecules that were then used to form complete molecular

fragments that appropriately represented the desired structures, as shown in Fig. 2. These molecular-fragment models were then used to conduct the MO-based DFT and TDDFT calculations. The structures of **1A** and **1B**, where X = Y = Cl, contained 88 atoms and consisted of four cations and four anions (represented by chlorine atoms), while those of **2A** and **2B**, where X = H₂O and Y = *p*-tosylate, contained 118 atoms and consisted of two cations and four anions (represented by *p*-toluenesulfonate). The ratio of anions to cations is dependent on the chemical structure of each complex.

The LANLD2Z ECP basis set⁴⁹ was used for ruthenium, while the 6-31G(d,p) set was used for all other atoms except hydrogens, which were modeled using the 3-21G(p) set. This setup was chosen due to the size of the structures, with heavier basis sets resulting in extremely slow geometry optimizations. The lighter basis set for the hydrogen atoms was employed since they have little to no influence on the overall optical properties of these materials. The structures of all complexes were modeled with the B3LYP functional⁵⁰ with the Grimme-D3 approach⁵¹ to account for the van der Waals forces.

Owing to the size and complexity of these structures, geometry optimization was conducted in piecewise steps, with only the final step having all atoms unconstrained. This optimization procedure used the DRIVER module with default convergence parameters for all except for the light-induced states of **2B** where the loose convergence parameters were required for the final unconstrained optimization. Breaking down each structural model into smaller blocks reduced the number of degrees of freedom, making it computationally simpler to optimize. In common with the PW-based-models, this was the case for all structures of the complexes except for the η^2 -(OS)O conformer in **1B** where the SO₂–Ru–Cl axis was fixed. The symmetry was maintained throughout the structural relaxations.

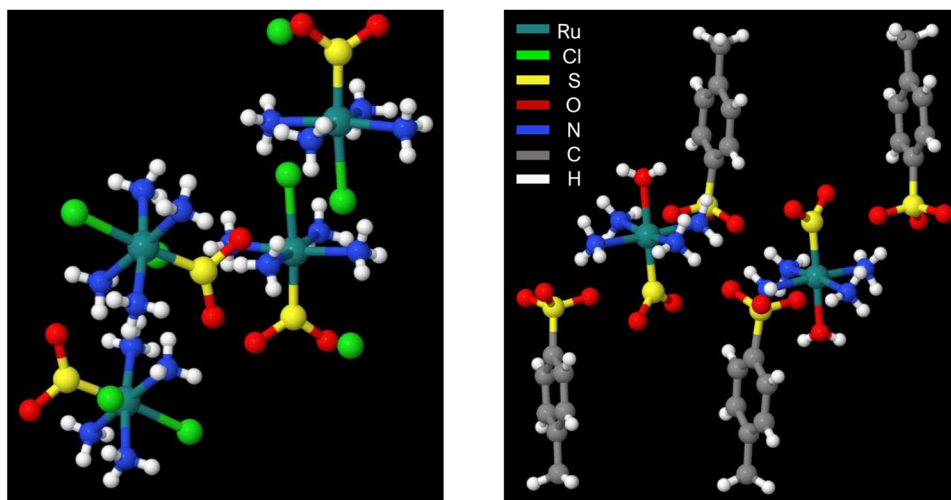


FIG. 2. Illustrations of the complete fragments used for the starting geometries of the dark states of **1B** (left) and **2B** (right). These fragments were built from the experimentally determined unit cell parameters and geometries.

B. Optical absorption spectra calculations via linear-response (LR)-TDDFT

1. Periodic models

The optimized geometries were then used to conduct TDDFT calculations in order to determine the optical absorption spectra via the *turbo_tddft* QE module.^{52,53} This module uses the Liouville–Lanczos approach⁵⁴ without computing empty states, which allows calculating absorption spectra across a wide frequency range. Significantly, TDDFT can only sample the gamma point for periodic systems. This is particularly difficult for bulk systems since they typically require a large Brillouin zone sampling to effectively simulate the optical response. This is usually the case for materials with high-energy excited states or charge-transfer states. To somewhat circumvent this issue, a supercell approach (much like that used for MO-DFT) is often employed for large bulk materials. However, we found that the performance of TDDFT in the periodic setup outperformed the supercell approach, and it was computationally less intensive due to the large amount of unoccupied space required in supercells. 5000 Lanczos iterations were used to calculate the full polarizability tensor and absorption coefficients for each structure.

2. Molecular-fragment models

As with periodic models, the optimized geometry of each structure was used as the starting point to calculate the singlet excited states and thus the optical absorption spectra of each complex via TDDFT. The same functional (B3LYP) and basis sets used for the structural optimization were also used to conduct the TDDFT calculations. The random phase approximation⁵⁵ was used throughout, with 30 states calculated for **1A** and **1B** and 20 states calculated for **2A** and **2B**. These calculations also gave access to the optical transitions involved.

C. Provision of experimental data

Dark- and light-induced crystal structures for both subject complexes^{14,26} were determined using photocrystallographic data, which had been collected at a N₂-based temperature using visible light. The temperatures and wavelengths varied according to the following conditions: 90(1) K, $\lambda = 488$ nm for **1A**;¹⁴ 100(2) K, $\lambda = 505$ nm for **1B**;²⁶ 90(1) K, $\lambda = 488$ nm for **2A**;¹⁴ and 13(2) K, broadband white light for **2B**.¹⁶ Single-crystal optical absorption spectra for **1** and **2** were acquired by Cole *et al.*^{26,55} using a custom-built experimental setup.²⁶

III. RESULTS

A. Optimized DFT-generated structural models

Before evaluating the DFT-optimized structures, it is important to assess the robustness of these models. Empirical studies have shown that the η^1 -OSO geometry is energetically the least stable, with the η^1 -SO₂ configuration naturally being the most stable. In general, this is observed for both techniques for all four structures of the two complexes except for the periodic model of **1B**, where calculations suggest that η^1 -OSO is the least stable conformer. Otherwise, for the periodic models, η^2 -(OS)O in **1A** is 2.62 eV above η^1 -SO₂ and η^1 -OSO in **1B** is 4.81 eV less stable than the η^1 -SO₂

isomer. Similarly, the η^2 -(OS)O configurations in both **2A** and **2B** are 1.37 eV higher than their corresponding dark-state η^1 -SO₂ isomers, with η^1 -OSO in **2B** being the least stable structure, 2.20 eV above the η^1 -SO₂ state. For the fragment models, in **1A** and **1B**, η^2 -(OS)O is 1.14 and 1.57 eV above that of the η^1 -SO₂ state, respectively, while η^1 -OSO in **1B** is 1.66 eV above that of the η^1 -SO₂ state. Likewise, in **2A**, η^2 -(OS)O is 0.33 eV above that of η^1 -SO₂, whereas in **2B**, it is 0.47 eV. η^1 -OSO in **2B** is 0.87 eV above its dark-state η^1 -SO₂ configuration and again is the least stable of the three structures.

As mentioned previously, the periodic models of **1B** did not display the expected trends. The modeled η^2 -(OS)O configuration is far less stable than that of the dark-state η^1 -SO₂ configuration, with its energy calculated to be even higher than that of the η^1 -OSO isomer. This can be explained by the fact that the η^2 -(OS)O isomer in **1B** is the only structure in which atomic constraints were required to successfully conduct geometry optimization. These constraints were necessary since unconstrained structural relaxation via both PW and MO methods resulted in the η^2 -(OS)O geometry transitioning to the η^1 -OSO state. Naturally, this meant that the η^2 -(OS)O state could not be minimized to the same extent as the η^1 -SO₂ or η^1 -OSO structures. Consequently, periodic models did not produce the expected stability trends, although the molecular-fragment models did. This difference is due to the nature of the two approaches. Owing to the periodic nature of the PW method, any changes in one region of a system naturally affect the entire system since the forces propagate throughout the structure. In contrast, MO DFT treats a system as one of finite molecules, where forces in one part of a system remain largely localized to that region; thus, in this case, the effects of fixing the Ru–SO₂–Cl axis had less of an impact. This is also presumably why the energy differences between the dark and light states are larger for the periodic models; for instance, the η^1 -OSO conformer in complex **1B** is 4.81 eV above that of the dark-state η^1 -SO₂ isomer, whereas for the fragment models, it is 1.57 eV above that of the dark state. It is important to note, however, that the PW self-consistent field calculations on the experimental geometries of complex **1B** (conducted before structural relaxation) did produce the expected trends.

Tables I and II present the selected bond lengths of the optimized geometries from all four structures of the two complexes. It is important to note that since hydrogen atoms are notoriously difficult to identify via x-ray crystallography, an idealized model was used to estimate their positions. This meant that one would expect that bonds that involve hydrogen to show the largest changes, which was indeed the case. The focus of this analysis is thus on the non-hydrogen bonds.

In general, the periodic models outperform their molecular-fragment counterparts, showing smaller deviations from the experimental geometries. Thus, as expected, the periodic nature of the PW method is more suited to models of these crystalline materials. Even though it uses very detailed basis sets and functionals, MO DFT still struggles since it is a finite method. While this can be somewhat offset by using a larger molecular fragment, this strategy is not feasible for such large systems. It can also be seen from both sets of models that the smallest changes are observed for the dark-state structures, whereas calculations on the light-induced η^2 -(OS)O and η^1 -OSO states show larger deviations from their experimental geometries. This can be explained by considering the way that DFT

TABLE I. Key bond lengths (Å) for structures of complex 1.

	Structure IA						Structure IB								
	η^1 -SO ₂			η^2 -(OSO)			η^1 -SO ₂			η^2 -(OSO) ^a					
	Expt.	PW	LCAO	Expt.	PW	LCAO	Expt.	PW	LCAO	Expt.	PW	LCAO	Expt.	PW	LCAO
Ru-S	2.0797(12)	2.07471	2.21132	2.323(16)	2.30202	2.46271	2.0702(17)	2.07460	2.21684	2.564(8)	2.56388	2.56388			
			2.22677			2.48203			2.15836						
			2.21132			2.46271			2.21711						
			2.22677			2.48203			2.18194						
Ru-O ₁				2.19(3)	2.11928	2.16454				2.369(14)	2.36794	2.36794	1.75(4)	1.93690	2.15558
						2.16731									2.01493
						2.16454									2.13299
						2.16731									2.01493
Ru-Cl _{trans}	2.4069(12)	2.39090	2.43521	2.322(11)	2.35273	2.39897	2.416(2)	2.39383	2.47146	2.367(18)	2.36776	2.36776	2.369(14)	2.33211	2.47767
			2.47630			2.40467			2.42480						2.39849
			2.43521			2.39897			2.46669						2.46575
			2.47630			2.40467			2.40745						2.39365
S-O ₁	1.451(3)	1.46969	1.48886	1.46(3)	1.54228	1.54583	1.441(4)	1.46857	1.48113	1.544(15)	1.54388	1.54388	1.14(4)	1.52881	1.52966
			1.48780			1.55709			1.49742						1.52667
			1.48886			1.54583			1.48044						1.51924
			1.48780			1.55709			1.48336						1.53341
S-O ₂	1.426(4)	1.46625	1.47594	1.41(6)	1.47803	1.51251	1.450(3)	1.46643	1.49554	1.23(5)	1.23256	1.23256	1.87(3)	1.47938	1.48489
			1.48878			1.48034			1.49326						1.50356
			1.47594			1.51251			1.48680						1.49042
			1.48878			1.48034			1.47917						1.49855

^aStructural relaxation for η^2 -(OSO) was conducted by fixing the SO₂-Ru-Cl_{trans} axis; hence, the PW and LCAO key bond lengths are the same as the experimental values.

TABLE II. Key bond lengths (Å) for structures of complex **2**.

	Structure 2A						Structure 2B								
	η^1 -SO ₂			η^2 -(OS)O			η^1 -SO ₂			η^2 -(OS)O			η^1 -OSO		
	Expt.	PW	LCAO	Expt.	PW	LCAO	Expt.	PW	LCAO	Expt.	PW	LCAO	Expt.	PW	LCAO
Ru-S	2.0892(5)	2.07406	2.17699	2.365(8)	2.31940	2.47012	2.0863(8)	2.07464	2.20640	2.481(14)	2.32302	2.41901	1.923(11)	1.92660	2.01445
Ru-O ₁	2.12825	2.11554	2.12861	2.034(15)	2.03567	2.06286	2.1312(15)	2.11531	2.26940	2.086(2)	2.04286	2.08925	2.086(2)	2.04198	2.13828
S-O ₁	1.4368(16)	1.46117	1.47631	1.487(17)	1.54273	1.55687	1.4451(14)	1.46143	1.47788	1.49(4)	1.53973	1.54856	1.514(10)	1.52573	2.18044
S-O ₂	1.4415(15)	1.46199	1.47300	1.436(17)	1.47872	1.49162	1.4431(14)	1.46206	1.47674	1.57(6)	1.47667	1.56092	1.426(15)	1.47863	1.52748
															1.48708

models the light states. Both η^2 -(OS)O and η^1 -OSO are modeled assuming 100% photoconversion, which stands in contrast to the experiment, where they coexist within a crystal lattice in various photoconversion fractions along with the residual dark-state η^1 -SO₂ configuration. This alters the surrounding environment and the LRES forces that are at play. It is thus not surprising that larger changes manifest where the SO₂ atoms are concerned, as this region is particularly influenced by crystal forces. This also explains why DFT struggles with the η^2 -(OS)O structure in **2**. Clearly, the crystalline environment that surrounds SO₂ in the experimental structure is crucial in keeping this geometry stable.

B. TDDFT-generated optical absorption spectral models

The top left and top right panels of Fig. 3 show the experimental optical absorption spectra for **1B** and **2A**, respectively, which have been published^{26,55} but are reproduced here for easy reference. It can be seen from the experimental optical absorption spectra that there are certain characteristics which are common to experimental spectra of both complexes, and in essence experimental spectra for all materials from this series of complexes. First, the transition from dark to light sees the absorption spectra broaden to encompass effectively the entire visible region (400–700 nm; 3.10–1.77 eV). The effect of light irradiation, and hence the formation of the light-induced states, is thus to raise the optical absorbance throughout the visible region, with the 500–700 nm region rising most significantly. It can thus be inferred that the major influence of the photoisomer formation lies in the lower-energy (red) region of the spectrum. Another important feature of these complexes is the extensive presence of metal-based charge transfer, although individual unique transfer bands are not easily distinguishable. It is also important to note that the experimental spectra for these complexes do not contain specific peaks. Rather, the comparison between experiment and computation will center on how well the TDDFT-generated spectra reproduce the above-mentioned spectral trends. The focus of this computational study is on the shape and coverage of the TDDFT-generated optical absorption spectra, particularly the differences between the spectra of the dark- and light-induced structures. Before the comparison between experiment and computation can be conducted, it is important to recognize that the experimental spectra for the light-induced structures is a combination of the optical response of any photoisomers that have been formed and any residual dark-state not having undergone photoisomerization. Hence, the light-induced experimental spectra of a complex must be compared to a *convolution* of the TDDFT-generated spectra of the dark-state and all photoinduced states of that same complex.

Figure 3 (middle panel) shows that the periodic-model spectra replicate these features relatively well. For all four structures of the two complexes, the overall optical absorbance increases from dark upon light induction, while the spectra become broader. Although not always in the desired region (400–700 nm or 3.10–1.77 eV), the spectra of the light-induced states are red-shifted as compared to those of their corresponding dark states, corroborating the experimental results that the photoinduced states are more influential in the lower-energy region of the spectrum when compared to the dark state. Spectra generated from the molecular-fragment models

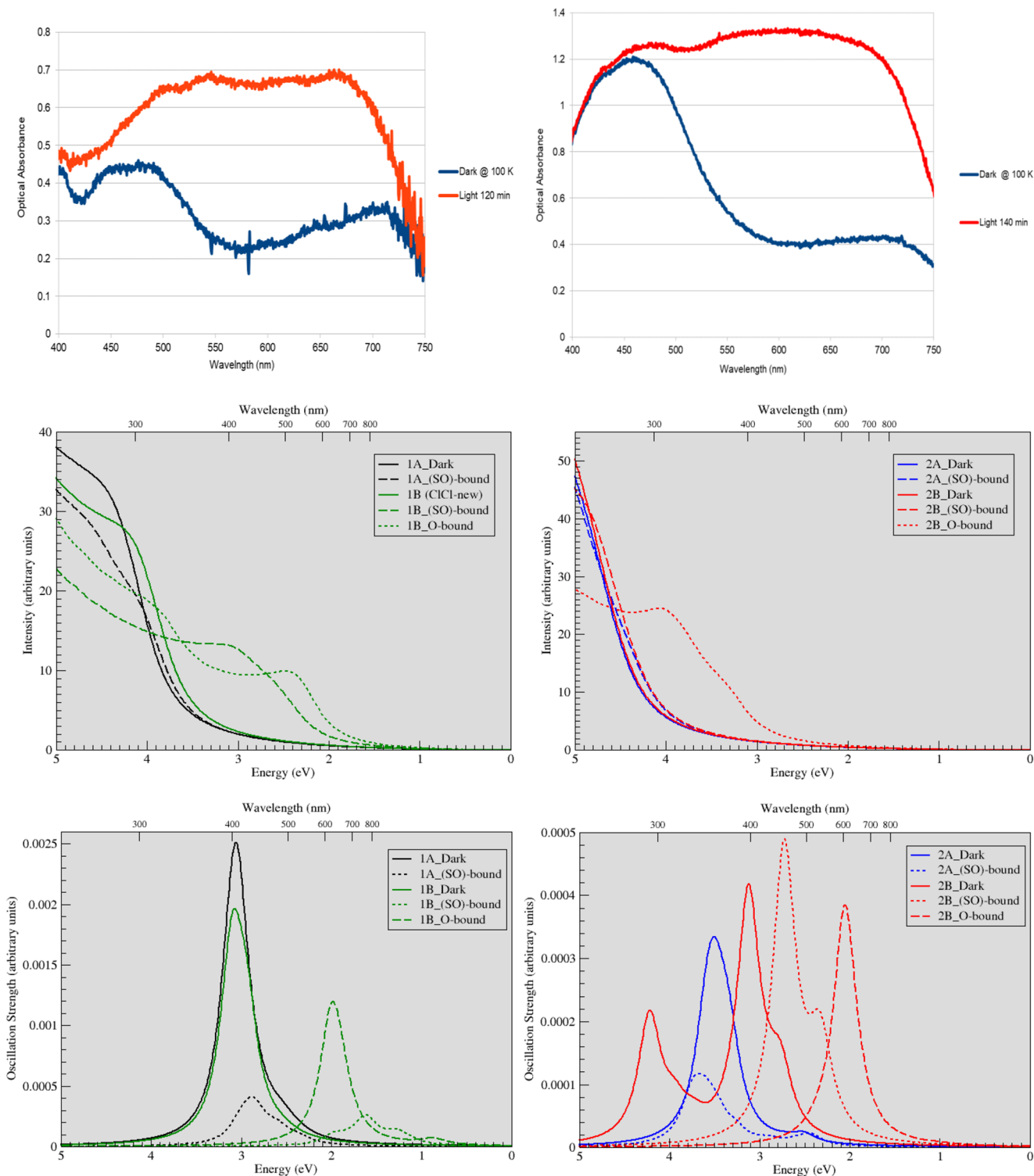


FIG. 3. Single-crystal optical absorption spectra for the dark- and light-induced states of (left) 1 and (right) 2 from (top) experimentally determined spectra,^{26,55} (middle) periodic models, and (bottom) molecular-fragment models. A Lorentzian broadening term of 0.3 eV was used for both periodic and molecular-fragment spectra. The experimentally determined single-crystal optical absorption spectra for 1 and 2 have been reproduced with permission from Cole *et al.*, *J. Phys. Chem. C* **124**(51), 28230–28243 (2020), and Cole *et al.* *RSC Adv.* **11**, 13183–13192 (2021), respectively.

(Fig. 3, bottom panel) also show much of the same trends, albeit that the transitions are slightly narrower when compared to the periodic-model spectra. This is likely to be due to the finite nature of MO methods and the fact that the molecular-fragment models cannot fully account for the periodicity of these complexes. As mentioned previously, the presence of light-induced states should broaden the spectra with contributions from the η^2 -(OS)O and η^1 -OSO states expected to be red-shifted when compared to their dark states, as seen for **1B** and **2B**. However, this is not the case for the molecular-fragment models of **1A** and **2A** where the inclusion of the light-induced state does not increase the optical absorbance. For both complexes, the η^2 -(OS)O spectral contribution lies within the spectra of the η^1 -SO₂ state, with the spectrum of the total photoinduced structure not broadening upon photoinduction, as seen in the periodic-model spectra for **1A** and **2A**. The spectra generated via PW-TDDFT therefore better reproduce the features seen in the experimentally determined optical absorption spectra. It is also worth mentioning that although both computational methods have spectra that do not fully lie in the desired energy range, they all fall well within 1 eV of the desired energy range. This is significant because optical absorption spectra for complicated materials are often manipulated via scissor functions or scaling factors to achieve desired results. This shows that PW-based periodic models can be used to effectively simulate optical properties of such large complicated extended systems for linkage photoisomerization studies.

However, some shortcomings of DFT are harder to overcome. As mentioned previously, DFT is well known to struggle when accounting for metal-based charge transfer and high-energy states. To this end, there are several instances of “gaps” in the TDDFT-generated spectra that indicate missing features. By comparison, experimental spectra show how the optical absorbance of the light-induced structures is more or less equal across the visible region, with the spectral features rising to a plateau shape. Although there are undoubtedly missing features in both TDDFT-generated spectral models, this shape is better reproduced by periodic models whose spectra are generally broader and seem to be able to access states across a larger energy range. In contrast, spectra for molecular-fragment models display marginally sharper peaks whose widths are insufficiently broad. This is not entirely surprising since periodic approaches can be more effective than MO-based methods at accessing high-energy states of a system.⁵⁶ This likely stems primarily from the finite nature of MO methods, as they are unable to truly appreciate the periodicity of extended materials. This can be somewhat compensated for by the use of appropriate molecular fragments that closely represent the extended system. However, in the case of the subject materials, this is unfeasible since these are large and intricate complexes. An extremely large molecular fragment would be needed, which would severely increase computational load. This then limits the appreciation of the LRES forces and intermolecular interactions that are inherent in these crystalline complexes, which contributes to the issues seen in the spectra that were calculated via the molecular-fragment model.

The shape of optical absorption spectra generated via molecular-fragment models is also affected, to some extent, by the choice of the *nroots* parameter. *Nroots* refers to the number of excited-state roots that are calculated. A larger number of roots

allow better access to a greater number of features that are present in the optical absorption spectrum of a system, particularly toward the higher-energy parts of the spectrum. This does not mean that high-energy states will suddenly become accessible since these failings are characteristic of the TDDFT method; yet, medium-energy states or relatively low-lying metal-based charge-transfer transitions may be revealed. For instance, the peak at 2.1 eV in the spectrum of **2B** that was generated via MO-based methods was not determined for a *nroots* value of 10, yet it became accessible when a value of 20 was selected. The minimum value of the *nroots* parameter that is required to access such states is characteristic of each complex since it will depend on its chemical nature (ligand **X**; counterion **Y**). The choice of the *nroots* parameter is easily deduced when experimental data are available for comparison, but it becomes difficult to validate when this is not the case. Thus, MO-based optical property calculations can be somewhat arbitrary. If sufficient experimental data are available for a large set of complexes, then the *nroots* value can become a “tunable” parameter; however, this is usually an exhaustive endeavor.

Periodic DFT-based methods are more robust and can be a more effective approach particularly when limited experimental data are present. For instance, if experimentally obtained optical absorption spectra are only available for a small set of complexes, their periodic DFT-model spectra can be used as a baseline to which “new” predicted spectra can be compared and characterized. Once a sufficiently large dataset of experimental spectra becomes available, PW and MO methods can be used in tandem to study these complexes more effectively. PW methods could be used in extensive large-scale studies for screening purposes after which spectra could be studied further with MO methods.

C. MO-based optical transitions

While PW-based TDDFT methods thus offer the better approach for predicting the spectral form, MO TDDFT calculations have an advantage over them in one important regard: they provide relatively easy access to the optical transitions and excited-state information of a complex. Since the subject complexes are large, complicated crystal structures with many heavy atoms, the distinguishability of their various transitions and understanding their effects is not straightforward. However, comparisons between the complexes in their dark- and light-induced states can still be very insightful. The focus here has been on the “major” transitions, i.e., those that we define as contributing at least 10% toward a photoinduced state.

Looking at the dark-state η^1 -SO₂ configuration of **1A**, there are only two instances where there are significant contributions from other atoms: the large peak just above 3 eV also has contributions from the Cl_{counterion} p-orbitals and to a lesser extent the photoactive sulfur s-orbitals. As expected, the unfilled ruthenium d-orbitals provide the dominating contributions to the spectra with no counterion contributions in the visible region. This is also the case for the dark-state η^1 -SO₂ configurations of **1B**, **2A**, and **2B**. The simulated spectra for these complexes show that any contributions from the non-ruthenium atoms, particularly counterions, occur at the higher-energy end of the spectra, with the visible region being dominated by the contributions from the unfilled ruthenium d-orbitals, as expected.

The story is not as straightforward for the light-induced spectra, as they show greater contributions from the non-ruthenium atoms, particularly the counterions. This is the case for both complexes with the exception of the photoinduced structures of **1B** where the spectra for both the η^2 -(OS)O and η^1 -OSO configurations are almost exclusively dominated by the unfilled ruthenium d-orbitals. In contrast, the spectrum for the η^2 -(OS)O structure of **1A**, although mostly dominated by ruthenium d-orbital-based transitions, does show counterion contributions from the chloride ions. The spectra for photoinduced structures of **2A** and **2B** show yet greater contributions from the counterions as compared to **1A** and **1B**, with the light-induced states in **2B** even displaying counterion contributions in the visible region. This is surprising since the visible region of the spectrum should be dominated by Ru-based transitions. Furthermore, as is known from its optical nature, *p*-tosylate should not be displaying transitions in the visible region. This showcases the shortcomings of using a finite method such as MO-DFT, as it is unable to truly appreciate the nature of extended materials, particularly those with intricate crystallographic forces at play. It is particularly susceptible to such misunderstandings for larger counterions, which is why these contributions were present for the structures in **2**, since the *p*-tosylate counterions are substantially larger and more influential than the chloride ions of **1**.

A proper understanding of the highly influential LRES forces present in such large periodic structures is a necessity to effectively model such materials. This illustrates the benefits of using a periodic methodology. Although MO-DFT offers more degrees of freedom due to a large variety of available Gaussian basis sets available, periodic methods are inherently designed to take such effects into account and represent a more intuitive way to treat this series of Ru-based photosensitive crystal materials.

IV. DISCUSSION

It can be seen that both periodic and molecular-fragment methodologies have performed relatively well in modeling the optical properties of these large periodic structures and have, especially for periodic methods, managed to replicate a lot of the features of the experimental optical absorption spectra despite the innate methodological limitations of TDDFT. It is important to try and understand what allowed TDDFT to succeed.

First, the structures of the subject complexes are not sensitive to a large sampling of the *k*-space. In general, the use of a dense *k*-point mesh allows for a more detailed analysis of optical properties, resulting in more features and characteristics of the optical response of the periodic system to be calculated. Techniques such as GW/BSE have this capability, whereas PW-TDDFT is limited to only sampling the gamma point when calculating broad range optical absorption spectra. Although the use of more *k*-points in a TDDFT model does not correct for its inherent limitations, it does allow for higher-quality spectra to be produced. Optical studies of periodic systems via PW-TDDFT are generally conducted using suitable supercells in order to circumvent this problem, yet this is not viable for such large systems as the subject complexes. The use of supercells was not necessary when modeling the subject complexes since they are not *k*-space sensitive. Fortunately, sampling the gamma point still allowed for good calculations of the optical response. PW-TDDFT would not have been an appropriate choice had these

complexes been more sensitive to sampling of the *k*-space. Access to high-quality experimental data also allowed for careful validation of these computational results.

Second, the most significant feature of these complexes is that they form long-lasting metastable photoinduced states. TDDFT particularly struggles with excitonic effects and high-energy excited states, such as charge transfer or Rydberg states, due to the lack of a long-range term in standard exchange-correlation functionals. Metastable states can be low-lying excited states or, as in the subject case, ground states, given that they have a distinct chemical structure and bonding compared to that of their dark-state configuration. This makes the subject complexes far more accessible to TDDFT-based methods, and this is why PW-TDDFT was selected to model these systems.

On a related point, TDDFT is often overlooked for optical studies due to the assumption that it will inherently fail for large periodic systems. However, the limitations of TDDFT, where high-energy states, metal-based charge transfer, or excitonic effects prevail, do not manifest themselves in the same way for every system. The mere presence of one or more of these electronic characteristics does not render TDDFT totally unusable; one simply has to be wary of what features can be successfully simulated. The performance of TDDFT will vary depending on the nature of the electronic states of the system at hand. Evaluating the attributes of these electronic states as a first step thus becomes crucial.

V. CONCLUSIONS

Optical properties of large intricate periodic systems are notoriously difficult to simulate, given that such systems are characterized by complicated periodic phenomena. DFT and TDDFT are the “go-to” techniques used to model these systems, with the molecular-orbital (MO)-based approach, intended for finite molecules, being the most commonly used method. However, the periodic nature of these systems must be considered if they are to be modeled effectively. Plane-wave (PW)-DFT is designed to treat extended periodic systems; yet, it is often overlooked when optical properties are concerned.

This study has compared the performance of periodic and MO-based DFT approaches to successfully model a set of large ruthenium-based photosensitive crystal complexes that have a rare ability to form long-lasting metastable states upon photoinduction. Structural relaxation calculations were conducted for all four structures of the two complexes using experimentally determined crystal structures as starting geometries. The DFT-optimized geometries were then used to calculate optical absorption spectra via linear-response-TDDFT. MO-based DFT also allowed for the analysis of the optical transitions involved, with a specific focus on the orbital contributions toward different features in the optical absorption spectra.

In general, the periodic models have been shown to be more effective in modeling these complexes, outperforming the molecular-fragment models. Periodic models have better replicated experimentally determined structural parameters, showing smaller deviations between calculated and experimental bond lengths. Periodic models are also more effective in simulating the features from experimentally determined single-crystal optical absorption spectra; whereby the light-induced states show better coverage over the

desired visible region of the spectra and a greater appreciation of the metal-based charge-transfer character that exists in these complexes. Periodic models are also more robust, given that the quality of the molecular-fragment-based spectra strongly depends on the number of states considered, which is difficult to assess for systems with no experimental data for comparison. Nonetheless, MO-based methods do allow for easier access to optical transitions and excited-state properties; they also reveal greater contributions for the counterions to the light-state spectra than that of the dark states of the subject complexes. With more experimental data, this analysis could be even more fruitful, allowing for a detailed analysis of specific regions of interest, and there are merits to using the two TDDFT methods together. However, periodic models have generally been more effective in modeling these large extended systems while providing a level of computational savings similar to that offered by molecular-fragment models. Periodic models should thus be considered as a more than viable alternative to conduct optical studies of large periodic systems. For investigations into linkage-photoisomerization processes, this study has also illustrated the possibility of using TDDFT to effectively model large complex periodic systems, something that has hitherto been considered to be highly unlikely, if the excited states and electronic properties can be considered by the kernel chosen. It is thus crucial to initially try to understand the nature of the photoinduced states of the system at hand to determine the appropriate methodology that offers both accuracy and computational feasibility.

SUPPLEMENTARY MATERIAL

See the [supplementary material](#) for the PW functional and pseudopotential benchmarking, and DFT-optimized geometries for complexes **1** and **2** for both LCAO MO-DFT-based (molecular-fragment) models and PW-DFT based (periodic) models.

ACKNOWLEDGMENTS

J.M.C. acknowledges the BASF/Royal Academy of Engineering Research Chair in Data-Driven Molecular Engineering of Functional Materials, which is partly supported by the STFC via the ISIS Neutron and Muon Source. J.M.C. also acknowledges Argonne National Laboratory for computational resources, where the work done was supported by the U.S. Department of Energy (DOE) Advanced Scientific Computing Research (ASCR) Leadership Computing Challenge (2020–2021) and the U.S. Department of Energy (DOE) Office of Science, Office of Basic Energy Sciences; and used research resources of the Center for Nanoscale Materials and the Argonne Leadership Computing Facility, Office of Science User Facilities operated for the DOE Office of Science by Argonne National Laboratory, supported by the U.S. DOE, all under Contract No. DE-AC02-06CH11357.

AUTHOR DECLARATIONS

Conflict of Interest

The authors have no conflicts to disclose.

Author Contributions

A.J. and J.M.C. conceived and designed the project. A.J. performed all of the calculations and associated data analysis, under

the Ph.D. supervision of J.M.C. A.V.-M. and M.G.S. provided assistance with the high-performance computing needs of the project. A.J. drafted the manuscript with assistance from J.M.C. All authors provided input to and agreed on the final manuscript.

DATA AVAILABILITY

The data that support the findings of this study are available within the article and its [supplementary material](#).

REFERENCES

- 1 T. Liu, F. Pagliano, R. van Veldhoven, V. Pogoretskiy, Y. Jiao, and A. Fiore, “Integrated nano-optomechanical displacement sensor with ultrawide optical bandwidth,” *Nat. Commun.* **11**, 2407 (2020).
- 2 J. Bochmann, A. Vainsencher, D. D. Awschalom, and A. N. Cleland, “Nanomechanical coupling between microwave and optical photons,” *Nat. Phys.* **9**, 712–716 (2013).
- 3 J. M. Abendroth, O. S. Bushuyev, P. S. Weiss, and C. J. Barrett, “Controlling motion at the nanoscale: Rise of the molecular machines,” *ACS Nano* **9**, 7746–7768 (2015).
- 4 F. Tong, W. Xu, T. Guo, B. F. Lui, R. C. Hayward, P. Palfy-Muhoray, R. O. Al-Kaysi, and C. J. Bardeen, “Photomechanical molecular crystals and nanowire assemblies based on the [2+2] photodimerization of a phenylbutadiene derivative,” *J. Mater. Chem. C* **8**, 5036–5044 (2020).
- 5 R. O. Al-Kaysi, F. Tong, M. Al-Haidar, L. Zhu, and C. J. Bardeen, “Highly branched photomechanical crystals,” *Chem. Commun.* **53**, 2622–2625 (2017).
- 6 P. Naumov, D. P. Karothu, E. Ahmed, L. Catalano, P. Commins, J. Mahmoud Halabi, M. B. Al-Handawi, and L. Li, “The rise of the dynamic crystals,” *J. Am. Chem. Soc.* **142**, 13256–13272 (2020).
- 7 P. Naumov, S. Chizhik, M. K. Panda, N. K. Nath, and E. Boldyreva, “Mechanically responsive molecular crystals,” *Chem. Rev.* **115**, 12440–12490 (2015).
- 8 S. O. Sylvester and J. M. Cole, “Solar-powered nanomechanical transduction from crystalline molecular rotors,” *Adv. Mater.* **25**, 3324–3328 (2013).
- 9 S. O. Sylvester, J. M. Cole, P. G. Waddell, H. Nowell, and C. Wilson, “SO₂ phototriggered crystalline nanomechanical transduction of aromatic rotors in tosylates: Rationalization via photocrystallography of [Ru(NH₃)₄SO₂X]₂tosylate₂ (X = pyridine, 3-Cl-pyridine, 4-Cl-pyridine),” *J. Phys. Chem. C* **118**, 16003–16010 (2014).
- 10 J. M. Cole, D. J. Gosztola, J. d. J. Velazquez-Garcia, S. Grass Wang, and Y.-S. Chen, “Rapid build up of nano-optomechanical transduction in single crystals of a ruthenium-based SO₂ linkage photoisomer,” *Chem. Commun.* **57**, 1320–1323 (2021).
- 11 J. M. Cole, J. d. J. Velazquez-Garcia, D. J. Gosztola, S. G. Wang, and Y.-S. Chen, “Light-induced macroscopic peeling of single-crystal driven by photoisomeric nano-optical switching,” *Chem. Mater.* **31**, 4927–4935 (2019).
- 12 S. O. Sylvester and J. M. Cole, “Quantifying crystallographically independent optical switching dynamics in Ru SO₂ photoisomers via lock-and-key crystalline environment,” *J. Phys. Chem. Lett.* **4**, 3221–3226 (2013).
- 13 S. O. Sylvester, J. M. Cole, and P. G. Waddell, “Photoconversion bonding mechanism in ruthenium sulfur dioxide linkage photoisomers revealed by in situ diffraction,” *J. Am. Chem. Soc.* **134**, 11860–11863 (2012).
- 14 A. Yu. Kovalevsky, K. A. Bagley, and P. Coppens, “The first photocrystallographic evidence for light-induced metastable linkage isomers of ruthenium sulfur dioxide complexes,” *J. Am. Chem. Soc.* **124**, 9241–9248 (2002).
- 15 A. Yu. Kovalevsky, K. A. Bagley, J. M. Cole, and P. Coppens, “Light-induced metastable linkage isomers of ruthenium sulfur dioxide complexes,” *Inorg. Chem.* **42**, 140–147 (2003).
- 16 K. F. Bowes, J. M. Cole, S. L. G. Husheer, P. R. Raithby, T. L. Savarese, H. A. Sparkes, S. J. Teat, and J. E. Warren, “Photocrystallographic structure determination of a new geometric isomer of [Ru(NH₃)₄(H₂O)(η¹-OSO)] [MeC₆H₄SO₃]₂,” *Chem. Commun.* **2006**, 2448–2450.
- 17 A. E. Phillips, J. M. Cole, T. d’Almeida, and K. S. Low, “Ru–OSO coordination photogenerated at 100 K in tetraammineaqua(sulfur dioxide)ruthenium(II) (±)-camphorsulfonate,” *Inorg. Chem.* **51**, 1204–1206 (2012).

- ¹⁸A. E. Phillips, J. M. Cole, T. d'Almeida, and K. S. Low, "Effects of the reaction cavity on metastable optical excitation in ruthenium-sulfur dioxide complexes," *Phys. Rev. B* **82**, 155118 (2010).
- ¹⁹K. T. Mukaddem, J. M. Cole, K. A. Beyer, and S. O. Sylvester, "Local atomic structure in photoisomerized ruthenium sulfur dioxide complexes revealed by pair distribution function analysis," *J. Phys. Chem. C* **124**, 10094–10104 (2020).
- ²⁰A. E. Phillips, J. M. Cole, K. S. Low, and G. Cibin, "L_{2,3}-edge x-ray absorption near-edge spectroscopy analysis of photoisomerism in solid ruthenium-sulfur dioxide complexes," *J. Phys.: Condens. Matter* **25**, 085505 (2013).
- ²¹P. Coppens, D. V. Fomitchev, M. D. Carducci, and K. Culp, "Crystallography of molecular excited states. Transition-metal nitrosyl complexes and the study of transient species," *J. Chem. Soc., Dalton Trans.* **6**, 865–872 (1998).
- ²²J. M. Cole, "Single-crystal X-ray diffraction studies of photo-induced molecular species," *Chem. Soc. Rev.* **33**, 501–513 (2004).
- ²³J. M. Cole, "Photocrystallography," *Acta Crystallogr., Sect. A: Found. Crystallogr.* **64**, 259–271 (2008).
- ²⁴J. M. Cole, "A new form of analytical chemistry: Distinguishing the molecular structure of photo-induced states from ground-states," *Analyst* **136**, 448–455 (2011).
- ²⁵J. M. Cole, "Applications of photocrystallography: A future perspective," *Z. Kristallogr.* **223**, 363–369 (2008).
- ²⁶J. M. Cole, D. J. Gosztola, J. d. J. Velazquez-Garcia, and Y.-S. Chen, "Systems approach of photoisomerization metrology for single-crystal optical actuators: A case study of [Ru(SO₂)(NH₃)₂Cl]Cl," *J. Phys. Chem. C* **124**(51), 28230–28243 (2020).
- ²⁷L. González, D. Escudero, and L. Serrano-Andrés, "Progress and challenges in the calculation of excited states," *ChemPhysChem* **13**, 28–51 (2012).
- ²⁸P.-F. Loos, A. Scemama, and D. Jacquemin, "The quest for highly accurate excitation energies: A computational perspective," *J. Phys. Chem. Lett.* **11**, 2374–2383 (2020).
- ²⁹S. Albrecht, L. Reining, R. Del Sole, and G. Onida, "Ab Initio Calculation of Excitonic Effects in the Optical Spectra of Semiconductors," *Phys. Rev. Lett.* **80**, 4510 (1998).
- ³⁰M. Rohlfing and S. G. Louie, "Electron-Hole Excitations in Semiconductors and Insulators," *Phys. Rev. Lett.* **81**, 2312 (1998).
- ³¹G. Strinati, "Application of the Green's functions method to the study of the optical properties of semiconductors," *Riv. Nuovo Cimento* **11**, 1–86 (1988).
- ³²L. Hedin, "New method for calculating the one-particle Green's function with application to the electron-gas problem," *Phys. Rev.* **139**, A796 (1965).
- ³³A. Warshel and M. Levitt, "Theoretical studies of enzymic reactions: Dielectric, electrostatic and steric stabilization of the carbonium ion in the reaction of lysozyme," *J. Mol. Biol.* **103**, 227–249 (1976).
- ³⁴S. Aono and S. Sakaki, "QM/MM approach to isomerization of ruthenium(II) sulfur dioxide complex in crystal; comparison with solution and gas phases," *J. Phys. Chem. C* **122**(36), 20701–20716 (2018).
- ³⁵P. Hohenberg and W. Kohn, "Inhomogeneous Electron Gas," *Phys. Rev.* **136**, B864 (1964).
- ³⁶W. Kohn and L. J. Sham, "Self-Consistent Equations Including Exchange and Correlation Effects," *Phys. Rev.* **140**, A1133 (1965).
- ³⁷E. Runge and E. K. U. Gross, "Density-Functional Theory for Time-Dependent Systems," *Phys. Rev. Lett.* **52**, 997 (1984).
- ³⁸R. G. Parr and W. Yang, *Density-Functional Theory of Atoms and Molecules*, International Series of Monographs on Chemistry (Oxford University Press, 1994).
- ³⁹W. E. Pickett, "Pseudopotential methods in condensed matter applications," *Comput. Phys. Rep.* **9**, 115 (1989).
- ⁴⁰P. Giannozzi, S. Baroni, N. Bonini, M. Calandra, R. Car, C. Cavazzoni, D. Ceresoli *et al.*, "QUANTUM ESPRESSO: A modular and open-source software project for quantum simulations of materials," *J. Phys.: Condens. Matter* **21**, 395502 (2009).
- ⁴¹P. Giannozzi, O. Andreussi, T. Brumme, O. Bunau, M. Buongiorno Nardelli, M. Calandra, R. Car, C. Cavazzoni, D. Ceresoli, M. Cococcioni, N. Colonna, I. Carnimeo, A. Dal Corso, S. de Gironcoli *et al.*, "Advanced capabilities for materials modelling with QUANTUM ESPRESSO," *J. Phys.: Condens. Matter* **29**, 465901 (2017).
- ⁴²C. Adamo and V. Barone, "Toward reliable density functional methods without adjustable parameters: The PBE0 model," *J. Chem. Phys.* **110**, 6158 (1999).
- ⁴³J. Heyd, G. E. Scuseria, and M. Ernzerhof, "Hybrid functionals based on a screened Coulomb potential," *J. Chem. Phys.* **118**, 8207 (2003).
- ⁴⁴J. P. Perdew, A. Ruzsinszky, G. I. Csonka, O. A. Vydrov, G. E. Scuseria, L. A. Constantin, X. Zhou, and K. Burke, "Restoring the Density-Gradient Expansion for Exchange in Solids and Surfaces," *Phys. Rev. Lett.* **100**, 136406 (2008).
- ⁴⁵D. Hamann, "Optimized norm-conserving Vanderbilt pseudopotentials," *Phys. Rev. B* **88**, 085117 (2013).
- ⁴⁶S. Grimme, "Semiempirical GGA-type density functional constructed with a long-range dispersion correction," *J. Comput. Chem.* **27**, 1787 (2006).
- ⁴⁷H. J. Monkhorst and J. D. Pack, "Special points for Brillouin-zone integrations," *Phys. Rev. B* **13**, 5188 (1976).
- ⁴⁸E. Aprà *et al.*, "NWChem: Past, present, and future," *J. Chem. Phys.* **152**, 184102 (2020).
- ⁴⁹P. J. Hay and W. R. Wadt, "Ab initio effective core potentials for molecular calculations. Potentials for K to Au including the outermost core orbitals," *J. Chem. Phys.* **82**, 299 (1985).
- ⁵⁰A. D. Becke, "Density-functional thermochemistry. V. Systematic optimization of exchange-correlation functionals," *J. Chem. Phys.* **107**, 8554 (1997).
- ⁵¹S. Grimme, J. Antony, S. Ehrlich, and H. Krieg, "A consistent and accurate ab initio parametrization of density functional dispersion correction (DFT-D) for the 94 elements H-Pu," *J. Chem. Phys.* **132**, 154104 (2010).
- ⁵²O. S. Malcioglu, R. Gebauer, D. Rocca, and S. Baroni, "turboTDDFT—A code for the simulation of molecular spectra using the Liouville–Lanczos approach to time-dependent density-functional perturbation theory," *Comput. Phys. Commun.* **182**, 1744–1754 (2011).
- ⁵³X. Ge, S. J. Binnie, D. Rocca, R. Gebauer, and S. Baroni, "turboTDDFT 2.0—Hybrid functionals and new algorithms within time-dependent density-functional perturbation theory," *Comput. Phys. Commun.* **185**, 2080–2089 (2014).
- ⁵⁴*Fundamentals of Time-Dependent Density Functional Theory*, Lecture Notes in Physics Vol. 837, edited by M. Marques, N. Maitra, F. Nogueira, E. Gross, and A. Rubio (Springer, Berlin, Heidelberg, 2012).
- ⁵⁵J. M. Cole, D. J. Gosztola, and S. O. Sylvester, "Low-energy optical switching of SO₂ linkage isomerisation in single crystals of a ruthenium-based coordination complex," *RSC Adv.* **11**, 13183–13192 (2021).
- ⁵⁶A. R. Kshirsagar, C. Attaccalite, X. Blase, J. Li, and R. Poloni, "Bethe–Salpeter Study of the Optical Absorption of trans and cis Azobenzene–Functionalized Metal–Organic Frameworks Using Molecular and Periodic Models," *J. Phys. Chem. C* **125**(13), 7401–7412 (2021).